nanomaterials

MDPI

*Article*

# Evaluation of MC3T3 cells proliferation and drug release study from sodium hyaluronate-BDDGE patterned gel

**Sumi Bang[1], Dipankar Das[1, 2], Jiyun Yu[2] and Insup Noh[1, 2,*]**

[1]Convergence Institute of Biomedical Engineering and Biomaterials,

[2]Department of Chemical and Biomolecular Engineering, Seoul National University of Science of Technology, 232 Gongneung-ro, Nowon-gu, Seoul 139-743, Republic of Korea

*Correspondence: insup@seoultech.ac.kr; Tel.: +822-970-6603; Fax: +822-977-8317

Academic Editor: Dong-Wook Han

Received:

**Abstract:**

A pattern gel for tissue engineering has been fabricated using sodium hyaluronate (HA) as biopolymer, 1,4-butanediol diglycidyl ether (BDDGE) as crosslinking agent and sodium hydroxide (NaOH) as base. Molding technique has been employed, where PDMS mold acted as fabrication chamber. The ATR-FTIR, $^{13}C$ NMR and TGA analyses implied the formation of crosslinking between HA and BDDGE. The SEM analysis confirmed the formation of micro/nano-morphological pattern on the surface of the fabricated HA gel. The gel formation has been confirmed by the swelling study using water at 37 °C. The *in vitro* release of dimethyloxalylglycine (DMOG) from HA gel showed controlled release nature up to 7 days in water at 37 °C. The bolus delivery results exhibited that the patterned gel with DMOG demonstrates better MC3T3 cell migration on surface than NaB. For local delivery, the HA gel with either 300 μM NaB or 300 μM DMOG induced cell clusters, while, 150 μM concentration showed high cell proliferation only. It has been observed that the presence of NaB helps to form cell clusters, that signify its vital role for bone regeneration. The patterned HA gel exhibited osteogenic behavior in ALP and Runx2 studies, which indicates its better bone regeneration ability.

**Keywords:** Cell proliferation; bone regeneration; hyaluronate; MC3T3 cell; pattern

## 1. Introduction

Development of size and shape mimetic bio-hydrogels has opened advanced prospects in addressing challenges in tissue engineering like tissue architecture, vascularization and cell seeding [1]. Hydrogels are water-swollen, physically or chemically crosslinked polymers which are remarkable in regenerative tissue engineering because of their capability to mimic the physical characteristics of tissues and organs [2, 3]. One of the numerous advantages of hydrogels are their simple treating conditions, which allows cell encapsulation directly in the gel as well as excellent biocompatibility [2]. The capacity to seed or encapsulate cells within 3-dimensional network has distinct significance, because these substrates well replicate *in vivo* microenvironments than that of cell seeding on materials, cell encapsulation in hydrogel and control of cell fates [2, 4, 5].

For *in vitro* tissue engineering and scaffold designs, the precise spatial mechanism and association of cells is vital to characterize the appropriate microenvironment around the cells, simulating *in vivo* physical and chemical cues [6]. Cell–cell contact and tissue architecture are two main factors which regulate cell behavior [1]. Even though, in tissue engineered scaffolds, cells have

self-assemble capacity to recover essential features of their cell–cell interactions, many of the interactions are eternally disappeared in the time of tissue isolation and seeding processes [1]. Moreover, the homogeneous cell seeding throughout the scaffolds is quite difficult, because of presence of large number of cells in the border of scaffolds [1]. Consequently, the capability to control cell–cell interactions, proper tissue architecture, and uniform cell seeding may support for the formation of functional tissue. Microfabrication methods are noteworthy technique in tissue engineering as they can be employed to replicate structures (0.1–10 μm), to regulate the microenvironment of individual cells (10-400 μm), to control the structure of clusters of cells (> 400 μm), and to control the interactions between multiple cell clusters [1]. In this aspect, soft lithography method has been established to be an economical and effective process for patterning of bare glass [7-9] or metal-coated glass [10-12], and polystyrene materials to flexible polydimethylsiloxane (PDMS) materials [13,14], and biomaterials [15-17]. Soft lithography technique includes stamps fabricated from an elastomer or soft material like PDMS. The PDMS stamp can mark extracellular matrix (ECM), self-assembled monolayer (SAM) and hydrogel to print on materials [6, 18]. The well defined ECM micro-patterns showed significant effect on numerous imperative cell behaviours such as cell adhesion and spreading [19, 20], cell proliferation and differentiation [21, 22], cell polarity [23, 24], and migration [25, 26]. From past few years, the capability to engineer the characteristics of hydrogels like adhesiveness, stiffness, cell signaling potential, size and shape have allowed several new applications in tissue engineering [1]. A variety of biopolymers such as collagen, gelatin, hyaluronate, fibrin, alginate, agarose and chitosan have been employed to synthesize biopolymer hydrogels for tissue engineering [18, 27]. Among these biopolymers, hyaluronate gained great interest in tissue regeneration owing to its unique properties for example ubiquitous existence as natural extra-cellular matrix throughout the human body, and its physico-chemical and immune-neutral characteristics [18, 27]. The valuable properties led to development of various HA hydrogels, for biomedical applications such as dermal fillers [28, 29], cartilage regeneration [30, 31], nucleus pulposus regeneration [32], bone tissue engineering [33]. and wound healing [34].

In this study, a cross-linked, patterned HA hydrogel has been fabricated through nucleophilic addition reaction using sodium hyaluronate (HA) as biopolymer, 1,4-butanediol diglycidyl ether (BDDGE) as crosslinking agent and sodium hydroxide (NaOH) as base. The BDDGE has been choose because of the presence of two epoxy rings, where, neucleophilile can attack on both ends and crosslinking will happen in HA. Micro-patterning technique has been used to design micro/nano morphologies on gel surface, because of the easy and simple operation technique of molding process. Scanning electron microscopy (SEM) analysis confirmed the formation of uniform morphologies on the surface of gel. The HA-BDDGE patterned gel can release dimethyloxalylglycine (DMOG) in a controlled manner up to 7 days in distilled water at 37 °C. The effects of DMOG and sodium borate (NaB) and the ways of release study (bolus and local) on MC3T3 cell behaviours have been evaluated. It is observed that the NaB containing pattern gel showed cells clusters. The patterned HA gel with more than 100 μM NaB showed cells clusters at day 7. In cell proliferation study, the system with bolus drug delivery showed best cell proliferations at the concentrations of 100 μM NaB and DMOG individually. When the drugs are locally delivered in the patterned HA gel, cell proliferations lasted longer over time. When both drugs having concentrations of 150 μM and 300 μM individually, cell proliferations were more effective. However, the patterned HA gel with 600 μM DMOG and NaB induced cell clusters. The vital role of NaB for bone regeneration has been endorsed from the formation of cell clusters in presence of NaB in the media. It has also been noticed that when drugs were delivered locally, the HA-BDDGE patterned gel showed higher intensity of ALP and Runx2, indicating better bone regeneration ability. Finally, the biocompatible crosslinked HA-BDDGE pattern gel could be used in bone regeneration application.

## 2. Experimental

### *2.1 Materials*

Hyaluronic acid (HA) (MW: 575 kDa) was received as gift from Hanmi Pharmaceutical Co. (Pyeongtaek, Korea), 1,4-butanediol diglycidyl ether (BDDGE, MW: 202 Da), $\alpha$-MEM and sodium butyrate (NaB) were purchased from Sigma – Aldrich (St. Luis, MO, USA). Sodium hydroxide (MW: 40 Da) was purchased from Yakuri Pure Chemical Co. (Kyoto, Japan). Poly(dimethyl siloxane) (PDMS) (184 Sylgard) was purchased from Dow Corning (USA). While penicillin-streptomycin was purchased Lonza Korea (Switzerland), cell counting kit-8 (CCK-8) solution was bought from Dojindo Laboratories (Japan). Live & dead viability/cytotoxicity kit for mammalian cells was purchased from Invitogen (USA), and dimethyloxalylglycine (DMOG) was procured from Cyman Chemical (USA). Anti-RUNX2 antibody, Anti-HIF-1-alpha antibody, Anti-Beta Actin antibody, and Goat Anti- Mouse IgG H&L (HRP) were bought from Abcam (UK). Anti-osteocalcin antibody was delivered from Santa Cruz (USA). RIPA buffer, protease inhibitor, and phosphatase inhibitor were purchased from Sigma-Aldrich (USA).

### *2.2 Fabrication of sodium hyaluronate-BDDGE patterned gel (HA-BDDGE)*

Fabrication of HA-BDDGE patterned gel was performed using the same method reported in our previous paper [18]. Briefly, Sodium hyaluronate (0.18 g) was homogeneously mixed in 1 mL of 1 % NaOH solution (w/v %) using centrifuge at room temperature with 10,000 rpm speed for 2 h. Then, 72 μL of BDDGE was added and mixed with a spatula. After that, the mixture was transported into a 10 mL syringe, injected on the PDMS mold supported with Teflon-glass slide and kept 24 h for crosslinking and pattern formation. Afterwards, the cross-linked patterned gel was taken out from the PDMS mold and put in 100 % ethanol for 24 h to remove the unreacted reagents. Then, the patterned gel was immersed in phosphate buffered solution (PBS) solution for 3 days by exchanging the PBS solution after every 12 h. The gel was dried in lyophilizer at -75 ℃ for further characterizations.

### *2.3. Characterizations*

The ATR-FTIR spectra of sodium hyaluronate, BDDGE, and dried HA-BDDGE patterned gel were recorded using ATR-FTIR spectrometer (Model: Travel IR, Smiths Detection, USA) in the wavelength range of 650-4000 $cm^{-1}$. The $^{13}C$ NMR analyses of sodium hyaluronate and dried HA-BDDGE gel were executed in solid state, while BDDGE was done in liquid state with nuclear magnetic resonance (NMR) spectrometer (Model: DD2 700, Agilent Technologies-Korea, USA). The TGA analyses of sodium hyaluronate and dried HA-BDDGE gel were carried out using thermogravimetric analyzer (Model: DTG-60, Shimadzu, Japan) under nitrogen atmosphere. The scan rate was 5 °C/min. The surface morphology of sodium hyaluronate and dried patterned HA-BDDGE gel were observed by SEM (Model: SEM, TESCAN VEGA3, Tescan Korea). The DMOG release study was performed by UV-Vis spectrophotometer (Model: BioMATE 3, Thermo Scientific, USA).

### *2.4. Swelling study*

The % swelling of the HA-BDDGE patterned gel was evaluated gravimetrically. In brief, the pre-weighed dried patterned gel (2r = 1 cm) was immersed in 100 mL distilled water in room temperature (25 °C) for 6 h. After regular time interval (1 h), the patterned gel was taken out from distilled water and the surface water was blotted off by tissue paper. The patterned gel was then reweighed until equilibrium of their weight was achieved. The % swelling was calculated by the equation (1):

$$\text{Swelling } (\%) = \frac{\text{Weight of gel} - \text{Initial dried weight of gel}}{\text{Initial dried weight of gel}} \times 100 \quad (1)$$

### *2.5. DMOG loading in HA-BDDGE patterned gel and in vitro release study*

For DMOG loading inside the HA-BDDGE patterned gel, dried gel samples were immersed into 2 mL of 25 μM, 50 μM, and 100 μM DMOG solutions at room temperature for 2 days in a 12 well plate. After absorption of drug solutions, the gels were dried in lyophilizer at -75 ℃.

The release study was performed in distilled water (pH: 7). After 1 h, 3 h, 6 h, 12 h, 24 h, 72 h, 120 h and 144 h, aliquots were taken out and absorption was recorded by UV-Vis spectrophotometer (Model: BioMATE 3, Thermo Scientific, USA).

### *2.6. In vitro MC3T3 cell culture on the surface of HA-BDDGE patterned gel*

An osteoblast precursor cell line derived from Mus musculus (mouse) calvaria (MC3T3, 10 passage) was used for in vitro cell study. The HA-BDDGE patterned gel was sterilized by autoclave (AC-02, Jeio tech, Korea) for 24 h. Then, the MC3T3 cells at the density of 10,000 cells/cm$^2$ were cultured on the surfaces of patterned gel with/without drugs for 7 days. The $\alpha$-MEM media containing both 10 % fetal bovine serum (Gibco) and penicillin-streptomycin (100 unit/mL) was added in the 24 well plate and incubated with 5 % $CO_2$ at 37 °C.

Cell adhesion and proliferation were evaluated with the cell counting kit-8 (CCK-8, Dojindo, Japan) after seeding MC3T3 cells on the surface of the hydrogel. The cell number was counted by the CCK-8 assay with a microplate reader (Tecan, Australia). In brief, 100 μL CCK-8 solution was mixed with 900 μL of $\alpha$-MEM medium in a 15 mL tube. Afterwards, the culture media was removed and the mixed CCK-8 solution was put in the 24 well plate and incubated for 2 h with 5 % $CO_2$ at 37 °C. After 2 h, 100 μL medium was transferred into a 96 well plate and the optical density was measured at the wavelength of 450 nm by the microplate reader.

### *2.7. Live & Dead assay*

*In vitro* cell viability and adhesions of the HA-BDDGE patterned gel was observed with MC3T3 cells in the 24-well culture plate. Live & dead viability/cytotoxicity kit for mammalian cells was prepared according to the protocol suggested by the vendor (Invitrogen, USA). The 1.2 μL of 2 mM ethidium homodimer-1 (EthD-1) and 0.3 μL of 4 mM calcein AM was added into 600 μL PBS and used for live and dead assay. The solution was put in the well plate and incubated for 30 min with 5 % $CO_2$ at 37 °C. The images of the MC3T3 cells on the HA-BDDGE patterned gel was captured by a fluorescence microscope (Leica DMLB, Germany).

### *2.8. Alkaline phosphatase (ALP) activity assay*

Alkaline phosphatase activities were determined by measuring the amount of *p*-nitrophenol produced using *p*-nitrophenol phosphate substrate. Cell lysates were mixed with alkaline buffer solution and gently shaken for 10 min. ALP substrate was added at room temperature for 30 min. After that, the reaction was stopped with the addition of 0.05 (N) NaOH, the absorbance at 405 nm was read and compared with a standard curve prepared with *p*-nitrophenol standard solution.

### *2.9. Western blot analysis*

We measured protein expressions of hypoxia inducible factor (HIF)-1 alpha, Runx2, osteocalcin of MC3T3 cells in vitro cultured in the 24 well plate, the patterned hydrogel with/without drugs by using western blot assay. After loading MC3T3 cells at a density of 10,000 cells/cm$^2$, cell culture lasted for 7 days by employing medium with/without DMOG, NaB containing cell culture medium were employed. TBS washing was performed on the cell cultured samples and then RIPA (Radio-Immunoprecipitation Assay) buffer with protease and phosphatase inhibitors was loaded on each well and patterned samples. Cells were harvested from the surfaces by using cell scraper, transferred to a 1 mL microtube in cold and stored at 4 °C refrigerator for 30 min. Centrifuge was performed at by using 16,000 rpm at 4 °C for 20 min and then surface layer was transferred to a new microtube. Cell lysate was obtained by heating the cell solutions with Lammeli sample buffer at 95 °C for 5 min, and then transferred into poly(vinylidene fluoride) (PVDF) membrane after loading into DS-PAGE

gel. The PVDF membrane was blocked with 5% skim milk solution. Primary antibodies were grafted by incubating with anti-HIF1 alpha antibody, anti-RUNX2 antibody, anti-osteocalcin antibody, and then secondary antibodies were done by incubating with goat anti-mouse IgG connected with horse radish protein (HRP). After loading ECL solution in the PVDF membrane with secondary antibody, excitation of drugs were measured with X-ray film by using β-actin as a loading control.

### *2.10. Statistical analysis*

Data were expressed as mean ± standard deviation. Statistical significance was assessed with one-way and multi-way ANOVA by employing the SPSS 18.0 program (ver. 18.0, SPSS Inc., Chicago, IL, USA). The comparisons between two groups were carried out using a t-test. The samples were considered as significantly different when $p < 0.05$.

## 3. Results and Discussion

### *3.1 Fabrication of sodium hyaluronate-BDDGE patterned gel (HA-BDDGE)*

The hyaluronate-BDDGE gel was synthesized using sodium hyaluronate (HA) as biopolymer, BDDGE as crosslinking agent and NaOH as base. It is assumed that the base (NaOH) abstracts hydroxyl proton from HA and form negative charge over oxygen atom, which acted as nucleophile in the reaction media. The nucleophile attacks on the less hindered electrophilic center of the epoxide rings of BDDGE and opens the epoxide rings. Thus, two HA moieties react with two epoxide rings of BDDGE and form covalent bond between HA and BDDGE (Scheme 1). Hence, it is supposed that one BDDGE molecule can covalently crosslinked two HA molecules through nucleophilic addition reaction. For the formation of pattern gel, molding technique was used, where PDMS mold acted as fabrication chamber. The pattern formation in the gel was confirmed by SEM analysis which was described in the characterization section.

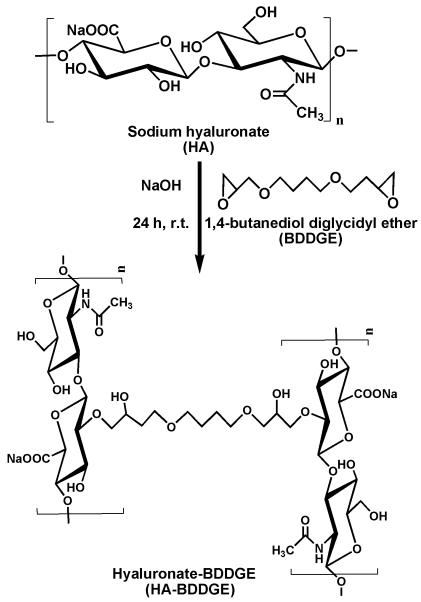


**Scheme 1.** Schematic representation of the reaction between HA and BDDGE

### *3.2. Characterizations*

Figure 1 represents the ATR-FTIR spectra of HA, BDDGE and dried HA-BDDGE gel. In the FTIR spectrum of sodium hyaluronate (HA, Figure 1a), the peaks at 3301, 2898, 1610, 1592, 1407 and 1038 $cm^{-1}$ are because of the stretching vibrations of O-H/N-H bond, C-H bond, C=O bond, amide-II, C-O bond of –COONa group and C-O-C bond, respectively [35]. The peaks at 1376 and 947 cm-1 are due to the vibrations of C-H bending and C-O-H deformation, respectively [35]. In the FTIR spectrum of BDDGE (Figure 1b), the characteristics peaks at 2927, 2865, 1253, 1100 and 908 $cm^{-1}$ are responsible

for C-H stretching of epoxy ring, C-H stretching -$CH_2$ bond, C-C bond, C-O-C stretching, and C-O stretching vibrations of epoxy ring, respectively [36]. While, in the FTIR spectrum of HA-BDDGE gel (Figure 1c), the peaks at 3317, 2924, 1608, 1562, 1405, 1374, and 946 $cm^{-1}$ are because of the stretching vibrations of O-H/N-H bond, C-H bond, C=O bond, amide-II, C-O bond of –COONa group, vibration C-H bending and C-O-H deformation, respectively. These peaks suggest the presence of HA moiety in the HA-BDDGE moiety. Again, the peaks for C-O-C stretching vibrations of HA and BDDGE moieties merged and gave a peak in the spectrum of HA-BDDGE gel with high intensity at 1036 $cm^{-1}$ (Figure 1c). Most importantly, the disappearance of the peak for C-O bond (908 $cm^{-1}$) of epoxy ring indicates the reaction between hydroxyl group of HA and epoxy ring of BDDGE (Figure 1c). Whereas, the increase of peak intensity at 3317 $cm^{-1}$ suggest the appearance of new free –OH groups due to the reaction between HA and BDDGE (Figure 1c and Scheme 1).

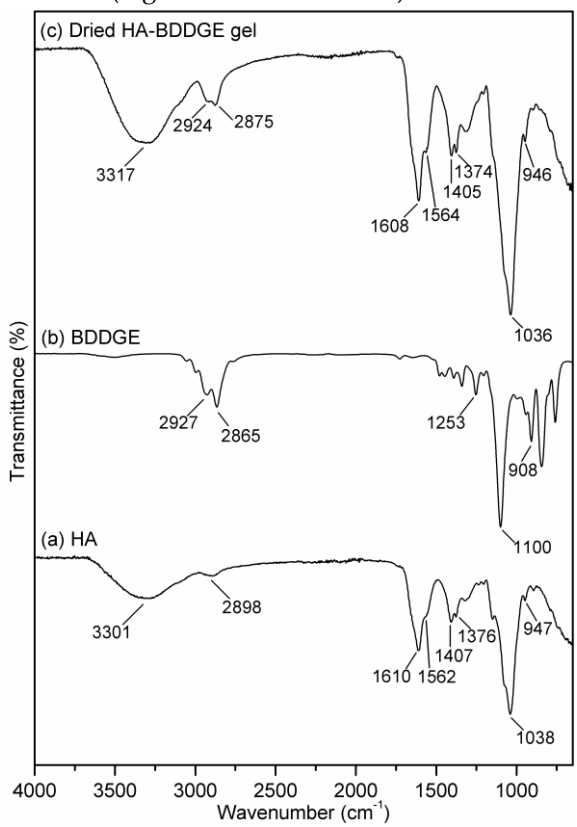


**Figure 1.** ATR-FTIR spectra of (a) HA, (b) BDDGE, and (c) dried HA-BDDGE gel

Figure 2 describes the $^{13}C$ NMR spectra of HA (solid state), BDDGE (liquid state), and dried HA-BDDGE gel (solid state). In the NMR spectrum of HA (Figure 2a), the chemical shifts at δ = 174.1, 103.8, 76.2 and 24.6 ppm are due to the presence of carbon atoms of C=O groups (C6, C7), anomeric position (C1, C1'), polysaccharide rings (C2-C5, C2'-C6') and -$CH_3$ group (C8), respectively [37]. In the NMR spectrum of BDDGE (Figure 2b), the sharp chemical shifts at δ = 44.8 and 51.5 ppm are owing to the carbon atoms of epoxy rings (C1, C1') and (C2, C2') respectively. While, the chemical shifts at δ = 25.2 and 70.9 ppm are because of the chain carbons (C5, C5') and (C3-4, C3'-4'), respectively (Figure 2b). In the NMR spectra, HA-BDDGE gel showed the chemical shifts at δ = 174.1, 101.9, 74.8, 71.4, 26.7 and 23.8 which are because of the carbon atoms of -C=O (C6, C7), anomeric position (C1, C1′), polysaccharide rings (C2-C5, C2'-C6'), C9-C12 positions, C13, and -CH3 group (C8), respectively (Figure 2c). The presence of characteristics peaks for C=O group and anomeric carbon (C1, C1′) and -CH3 group (C8) imply the presence of HA in the gel network (Figure 2c). While, the peaks for the carbons of C13 and between C9-C12 confirmed the presence of BDDGE in the gel network and successful formation of HA-BDDGE compound (Figure 2c).

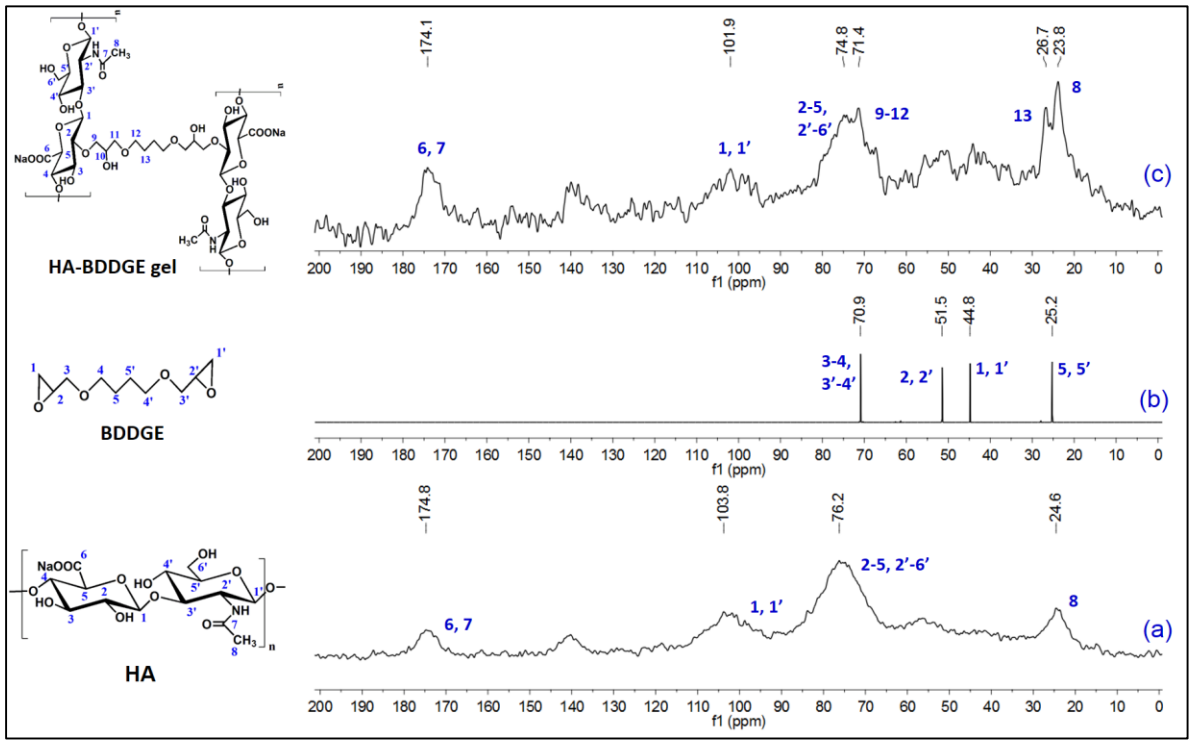


**Figure 2.** $^{13}$C NMR spectra of (a) HA (solid state), (b) BDDGE (liquid state), and (c) dried HA-BDDGE gel (solid state)

The thermal properties of HA and dried HA-BDDGE gel were analyzed by TGA and results are shown in Figure 3. A significant weight loss has been noticed for two samples between the temperature range of 50 - 520 °C because of the thermal breakdown of HA [38]. The initial weight loss of HA between 28 - 100 °C is owing to moisture evaporation (Figure 3). A sharp weight loss zone is seen between approximately 200 - 260 °C, then relatively slow decomposition is noticed up to 260 - 400 °C, and 400 - 700 °C which is owing to the complete breakdown of polysaccharide residue. The HA showed ~ 91.25 % weight loss in the TGA analysis (Figure 3). In the TGA plots HA-BDDGE gel, the first weight loss region (28 - 100 °C) is because of the evaporation of moisture (Figure 3). The steady second (160 – 310 °C), third (310 - 500 °C) and fourth (500 - 700 °C) weight loss zones are due to the decomposition of HA, BDDGE unit and completely breakdown of crosslinked network. The weight loss of HA-BDDGE gel was found as 69.67 %, which indicates that the covalent attachment between HA and BDDGE increased the thermal stability of the HA-BDDGE gel.

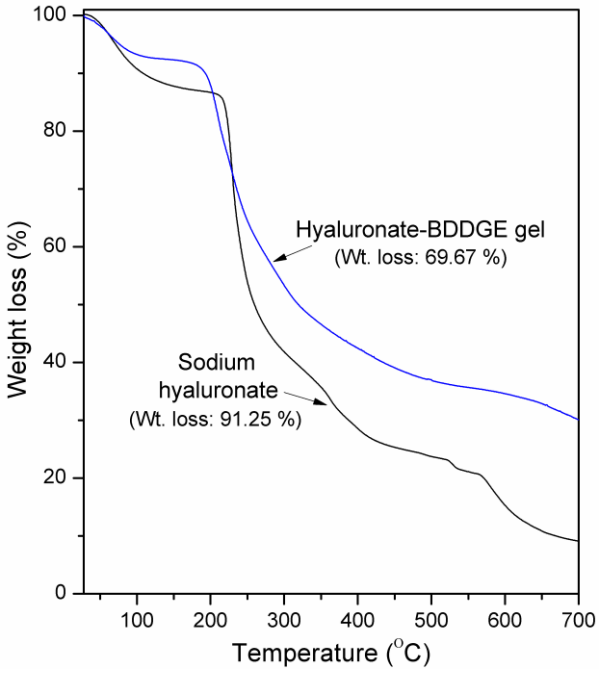


**Figure 3.** TGA plots of HA and dried HA-BDDGE patterned gel

Figure 4 depicts the SEM images of HA and dried HA-BDDGE patterned gel and its detailed characterizations of patterning gels has been reported in our previous report [18]. From Figure 4a, it is observed that sodium hyaluronate exhibits aggregated pod-like structure with rough morphology. After modification with BDDGE, the morphology of HA totally changed and the gel appeared with relatively smooth surface (Figure 4b). While, the pattern shape is clearly observed from the both surface (Figure 4b) and cross-section images (Figure 4c). It has also been noticed that the width of individual pattern is approximately 5 μm, whereas, the gap between two pattern (valley) is 15 μm (Figure 4b and c). Nano scale top of mountain of the pattern was observed at nano-levels (Figure 4c). It is expected that the regular distribution of pattern in the gel structure could be assisted for high adhesion and proliferation of cells.

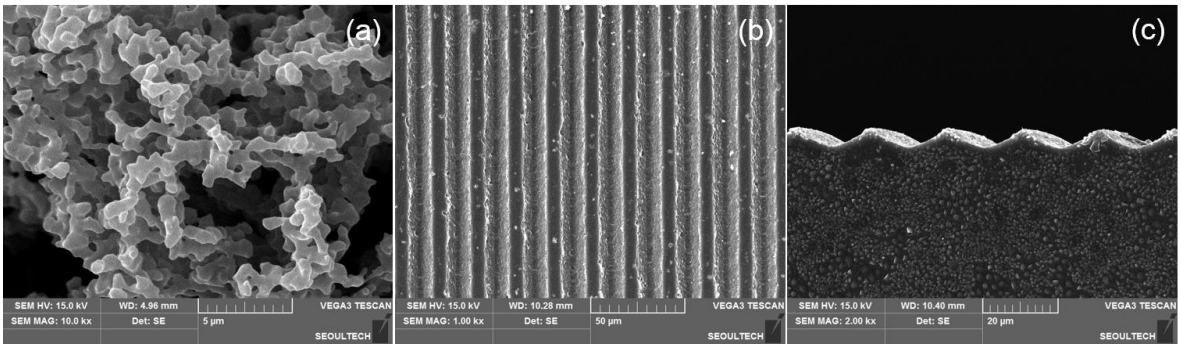


**Figure 4.** SEM images of (a) HA powder, (b) surface of HA-BDDGE patterned gel, and (c) cross-section of HA-BDDGE patterned gel.

### *3.3. Swelling study*

To confirm the gel property of the crosslinked HA-BDDGE polymer, swelling study was performed at distilled water and 37 °C. From the Figure 5a, it is obvious that the rate of water absorption by the HA-BDDGE polymer was higher in the initial stage, then it decreased and finally reached to equilibrium swelling state around at 5 h. The HA-BDDGE patterned gel demonstrated %

swelling as 439 ± 21 %. The swelling property confirmed the formation of hydrogel of crosslinked HA-BDDGE polymer in distilled water at 37 °C.

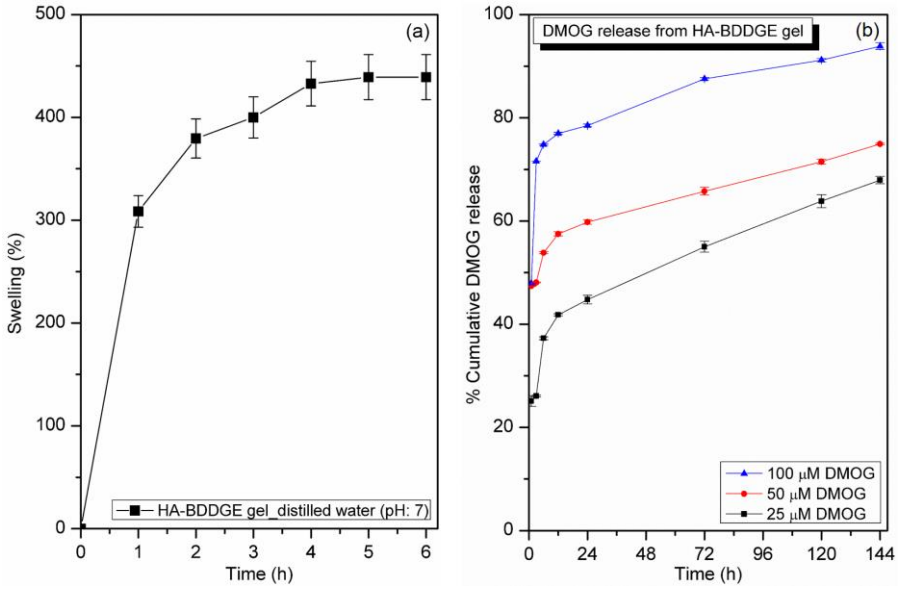


**Figure 5.** (a) Graph of % swelling *vs*. time for HA-BDDGE patterned gel in water, and (b) *in vitro* release profile of DMOG from loaded HA-BDDGE patterned gel over time

### *3.4. In vitro DMOG release from loaded HA-BDDGE patterned gel:*

The *in vitro* DMOG release behavior of DMOG loaded HA-BDDGE patterned gel with different concentrations of DMOG (25, 50 and 100 μM) is shown in Figure 5b. Release study was performed after the absorption of 25, 50 and 100 μM DMOG. Distilled water (pH 7.0) was as medium, the temperature was 37 °C. After 1 h, 3 h, 6 h, 12 h, 24 h, 72 h, 120 h and 144 h, the absorption of drugs in the aliquots was measured by UV-Vis spectrophotometer (Model: BioMATE 3, Thermo Scientific, USA). From the release profile (Figure 5b), it is apparent that the initial rate of DMOG release is higher compared to that of later stage. This is may be because of the higher rate of swelling of the HA-BDDGE patterned gel and the release of DMOG molecules present on the surface of gel at the initial period. However, after reaching the equilibrium swelling, the rate of drug diffusion decreased. Among three loaded HA-BDDGE patterned gels (25, 50 and 100 μM), the gel containing 100 μM DMOG exhibited highest rate of DMOG diffusion (Figure 5b). This is because of the existence of higher dose of DMOG than that of other grades in the reservoirs in diffusion system. In case of 100 μM grade, lesser amount of the percentage of HA polymer presents in the formulation compared to 25 and 50 μM system. Thus, the interaction with HA-BDDGE gel and DMOG will be to some extent weaker. Besides, the gel network from which drug molecules diffuse will be weaker and the rate of DMOG release will be faster. After 7 days, the % DMOG release from the HA-BDDGE patterned gel are measured as 93.8 ± 0.6 % (for 100 μM), 74.9 ± 0.1 % (for 50 μM), and 67.9 ± 0.9 % (for 25 μM).

### *3.5. In vitro MC3T3 cells study*

#### 3.5.1. Effect of drug molecules of cell proliferation

To observe the effects of DMOG and NaB release on cell response, 100 μM of NaB, DMOG and NaB/DMOG were bolus-delivered in 24 well plate after seeding 1 ×$10^5$ MC3T3 cells/well with media and the cell culture was lasted for 7 days. Cell counting was observed and measured at day 1, 3, 5, and 7 with light microscopy (Figure 6b) and CCK-8 assay (Figure 6a), respectively. Overall cell proliferation improved when drugs were delivered (Figure 6a-b). When normalized with the cells at day 1, cell proliferation rates were measured as 115 ± 2 % and 321 ± 34 % at day 3 and 7 on the well plate, respectively (Figure 6a). Importantly, when NaB were bolus-delivered, its cell proliferations

improved to 121 ± 2 % and 346 ± 33 % at day 3 and 7, respectively (Figure 6a). On the other hand, when DMOG were bolus-delivered, its cell proliferations improved to 136 ± 2 % and 354 ± 20 %, which are similar to those of NaB cases (Figure 6a). In the case of delivery of both NaB and DMOG at the same time, its cell proliferations were measured as 129 ± 2 % and 332 ± 14 % (Figure 6a). Hence, there were no significant differences in cell proliferation between drug species.

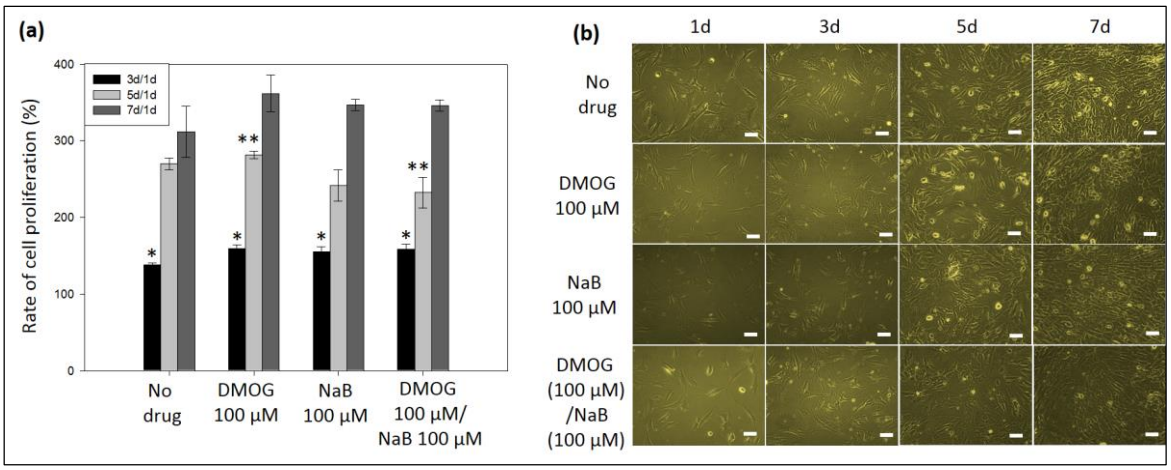


**Figure 6.** (a) Effect of bolus delivery of drugs (DMOG 100 μM, NaB 100 μM, NaB 100 μM + DMOG 100 NaB 100 μM) on MC3T3 cell proliferation on well plate, (b) images of MC3T3 cells on well plate by light microscopy (scale bar = 50 μm).

### 3.5.2. Effect of DMOG or NaB to MC3T3 cell proliferation cultured on the surface of HA-BDDGE patterned gel

To observe the effect of DMOG and NaB delivery onto MT3T3 cells cultured on the surface of HA-BDDGE patterned gel, cells were culture in native $\alpha$-MEM medium and the medium with 25 μM, 100μM, 400 μM DMOG and NaB drugs. The MT3T3 cells were seeded and *in vitro* cultured on the HA-BDDGE patterned gel at a density of 1 ×$10^5$/$cm^2$ for 7 days, where cellular behaviors and cell proliferation were observed with light microscopy, live and dead assay and CCK-8 assay, respectively (Fig. 7).

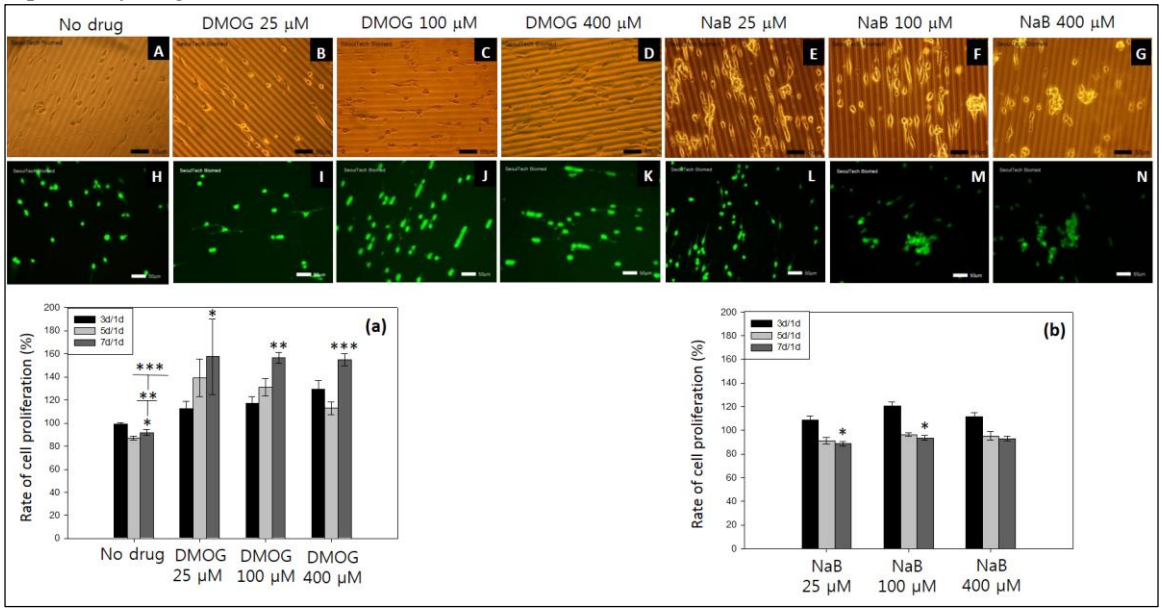


**Figure 7.** *In vitro* cellular behavior of MC3T3 cells on the surface of HA-BDDGE patterned gel in either absence or presence of DMOG and NaB in medium after 7 days: (A, H) No drug, (B, I) DMOG-25μM, (C, J) DMOG-100μM, (D, K) DMOG-400μM, (E, L) NaB-25μM, (F, M) NaB-100μM, (G, N) NaB-400μM, (scale bar = 50 μm), and proliferation of MC3T3 cells in absence or presence of (a) DMOG, and (b) NaB.

According to both LM and L/D assay, it is observed that all cells were alive after day 7 (Figure 7A-N). The NaB containing HA-BDDGE gel showed cells clusters. In specific, the patterned gel with 25μM NaB showed cell migration on surface (Figure 7E, 5L), whereas, the hydrogel with more than 100 μM NaB showed cells clusters even at day 7 (Figure 7F-N). The patterned gel with DMOG demonstrated better cell migration on surface than NaB (Figure 7B-K). The cell proliferation was measured using CCK-8 assay by normalizing the data of day 3, 5 and 7 by day 1. The patterned gel with DMOG showed initial quick cell proliferation at day 3 (Figure 7a), but their proliferations rate decreased when the concentrations of DMOG increased. There was no difference at day 7 (Figure 7a). The patterned gel with NaB showed similar trends in cell proliferation over time (Figure 7b).

### 3.5.3. Effect of DMOG and NaB to MC3T3 cell proliferation on the surface of HA-BDDGE patterned gel depending on the delivery mode

To detect the cell behaviors on the HA-BDDGE patterned gel with DMOG and NaB, the 12.5μM, 50μM, 100μM and 200μM of DMOG and NaB were added into the culture medium. $1 \times 10^5$ MC3T3 cells/cm$^2$ were employed for in vitro study for 7 days. The LM, LD, and CCK-8 tests were performed. For the effects of drugs on cell behaviors, drugs were loaded in gel (local delivery) and add in the medium (bolus delivery). According to LD assay results at day 7, the medium with both NaB and DMOG induced cell clusters on the patterned HA gel (Figure 8A-D and H-K). For local delivery, the HA gel with either 300 μM NaB or 300 μM DMOG induced cell clusters, but those with 150 μM showed high cell proliferation only, indicating the importance of the amount of drugs loaded for cell cluster formations (Figure 8E-G and L-N).

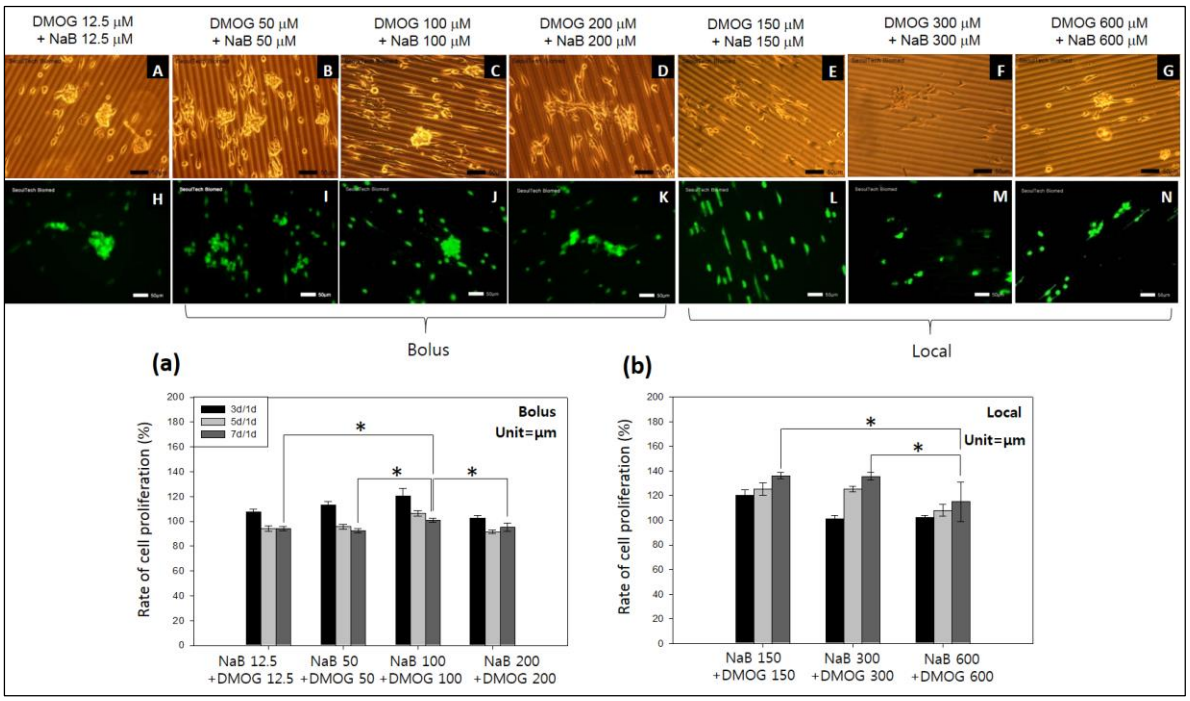


**Figure 8.** *In vitro* cellular behavior of MC3T3 cells on the surface of HA-BDDGE patterned gel in presence of both DMOG and NaB after 7 days: bolus delivery (A, H) NaB/DMOG 12. 5μM, (B, I) NaB/DMOG 50μM, (C, J) NaB/DMOG 100 μM, and local delivery (D, K) NaB/DMOG 150 μM, (E, L) NaB/DMOG 300μM, (G, N) NaB/DMOG 600 μM, and their corresponding proliferation results of MC3T3 cells (a) bolus, and (b) local delivery

For cell proliferation assays, the system with bolus drug delivery showed best cell proliferations at the concentrations of 100 μM NaB and DMOG individually (Figure 8a). When the drugs are locally delivered in the patterned gel, cell proliferations lasted longer over time. When both drugs having concentrations of 150 μM and 300 μM individually, cell proliferations were more effective (Figure 8b

and Figure 8E-F, L-M). However, the patterned gel with 600 μM DMOG and NaB induced cell clusters (Figure 8b and Figure 8G, N).

3.5.4. Cell cluster behaviours on the surface of HA-BDDGE patterned gel by bolus and local delivery of DMOG and NaB:

The cell clusters formation on the patterned HA gel were observed as shown in Figure 10. For bolus study 100 μM DMOG and NaB was added three times (100 μM × 3) during 7 days. The same amount of drug loaded gel was used for local delivery. The patterned gels either no drugs or DMOG showed no cell clusters. While, the presence of NaB helps the formation of clusters, indicating NaB has vital role for bone regeneration (Figure 9a-l).

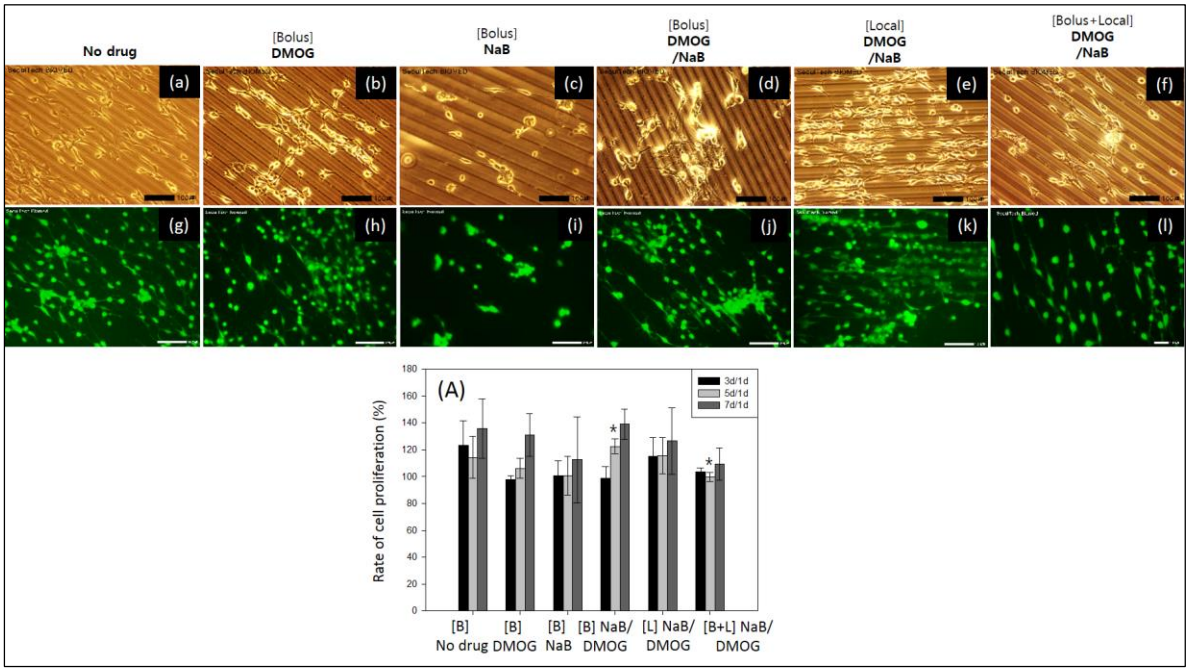


**Figure 9.** Cell cluster behaviours results: (a-l) Live and dead assay of cells on the HA-BDDGE patterned gel with and without the effects of local and bolus DMOG/NaB delivery, and (A) Corresponding cell proliferation of MC3T3 cells on the patterned HA gel measured by CCK-8 assay.

The NaB either in the medium or inside the patterned gel induced cell cluster (Figure 9). When NaB was introduced in medium cell area reduced and the cell clusters areas increased as the concentration increased. When we added both NaB and DMOG in the medium, cell surface area decreased more than only NaB, cell clusters were highest. On the other hand, the drugs were added inside the patterned gel, did not showed any significant trends. However, cell clusters were highest when 300 μM DMOG and NaB were added individually.

*3.6. Effect of drug molecules of osteogenic or angiogenic gene expressions response on cells*

The degree of protein expression was analyzed using western blot assay. The results are as shown Figure 10. The results showed that even though cell proliferation was low when drugs were delivered locally, the HA-BDDGE patterned gel showed higher intensity of ALP (Fig. 10a) than those of either no drug or bolus delivery of DMOG. There was no significant difference where drug was delivered in bolus. Expression of Runx2 increased when combination of 100 μM DMOG and 100 μM NaB was delivered in bolus (Fig. 10b), indicating better bone regeneration ability. In all cases hypoxia effects were not observed, judged from the data of HIF1-alpha in this experimental conditions (Fig 10b).

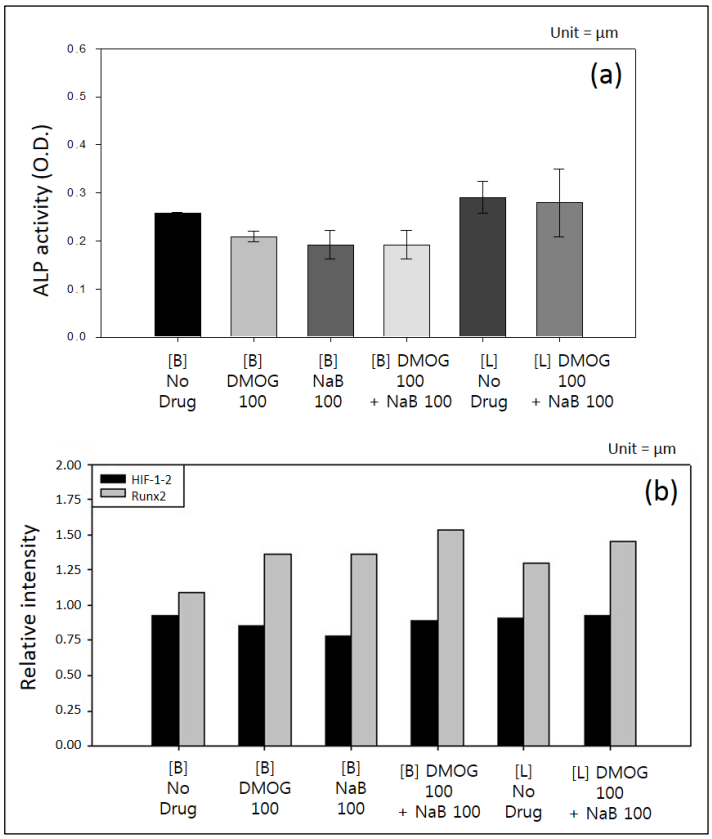


**Figure 10.** (a) Assays of alkaline phosphatase activity, (b) and expression of HIF-1 alpha and Runx2 by the delivery of with and with DMOG/NaB through bolus and local modes.

## 4. Conclusions

The cross-linked patterned HA-BDDGE gel has been successfully fabricated through nucleophilic addition reaction using NaOH as base. The chemical analyses such as ATR-FTIR, 13C NMR and TGA analyses implied the formation of crosslinked network. SEM analysis confirmed the micro/nano pattern architecture on the surface of the gel. The width of pattern was approximately 5 μm, while, the valley between two patterns was 15 μm. The gel attained equilibrium swelling state after ~5 h in distilled water at 37 °C, which confirmed its hydrogel nature. *In vitro* release study from DMOG-loaded HA-BDDGE patterned gel showed sustained release nature. In cell proliferation study, the system with bolus drug delivery showed best cell proliferations at the concentrations of 100 μM NaB and DMOG individually in this experimental conditions. When the drugs are locally delivered in the patterned HA-BDDGE gel, cell proliferations lasted longer over time. When both drugs having concentrations of 150 μM and 300 μM individually, cell proliferations were more effective. However, the patterned gel with 600 μM DMOG and NaB induced cell clusters. The cluster formation results suggested that the presence of NaB helps the formation of clusters, which indicates NaB has vital role for bone regeneration. It has been also noticed that when drugs were delivered locally, the HA-BDDGE patterned gel showed higher intensity of ALP and Runx2, indicating better bone regeneration ability. Finally, from the experiment evidences it is concluded that the crosslinked HA-BDDGE pattern gel could be used in bone regeneration application, by controlling mode of drug delivery.

## Acknowledgments:

This work was supported by the National Research Foundation of Korea (NRF) Grant (2014K2A2A7060928 and 2015R1A2A1A10054592).

## References


1. Khademhosseini, A.; Langer, R. Microengineered hydrogels for tissue engineering. *Biomaterials* **2007**, *8*, 5087-5092.
2. Khetan, S.; Burdick, J.A. Patterning hydrogels in three dimensions towards controlling cellular interactions. Soft Matter **2011**, *7*, 830-838.
3. Tibbitt, M.W.; Anseth, K.S. Hydrogels as extracellular matrix mimics for 3D cell culture. *Biotechnol. Bioeng*. **2009**, *103*, 655-663.
4. Kim E and Giyoong Tae G.; Direct reprogramming and biomaterials for controlling cell fate. *Biomater. Res.* 2**017**, *20*, 39.
5. Roberts J.J., Naudiyal, P., Lim K.S., Poole-Warren L. A. and Martens P. J., A comparative study of enzyme initiators for crosslinking phenol-functionalized hydrogels for cell encapsulation. *Biomater. Res* **2017**, *9*, 1772-1781.
6. Tang, X.; Ali, M.Y.; Saif, M.T.A. A novel technique for micro-patterning proteins and cells on polyacrylamide gels. *Soft Matter* **2012**, *8*, 7197-7206.
7. Nishizawa, M.; Takoh, K.; Matsue, T. Micropatterning of HeLa Cells on Glass Substrates and Evaluation of Respiratory Activity Using Microelectrodes. *Langmuir* **2002**, *18*, 3645-3649.
8. Thakar, R.G.; Ho, F.; Huang, N.F.; Liepmann, D.; Li, S. Cell-Shape Regulation of Smooth Muscle Cell Proliferation. *Biochem. Biophys. Res. Commun*. **2003**, *307*, 883-890.
9. Xia, N.; Thodeti, C.K.; Hunt, T.P.; Xu, Q.; Ho, M.; Whitesides, G.M.; Westervelt, R.; Ingber, D.E. Directional control of cell motility through focal adhesion positioning and spatial control of Rac activation. *FASEB J.* **2008**, *22*, 1649-1659.
10. Raghavan, S.; Chen, C.S. Micropatterned Environments in Cell Biology. *Adv. Mater*. **2004**, *16*, 1303–1313.
11. Whitesides, G.M.; Ostuni, E.; Takayama, S.; Jiang, X.; Ingber, D.E. Soft Lithography in Biology and Biochemistry. *Annu. Rev. Biomed. Eng.* **2001**, *3*, 335-373.
12. Falconnet, D.; Csucs, G.; Grandin, H.M.; Textor, M. Surface engineering approaches to micropattern surfaces for cell-based assays. *Biomaterials* **2006**, *27*, 3044-3063.
13. Gopalan, S.M.; Flaim, C.; Bhatia, S.N.; Hoshijima, M.; Knoell, R.; Chien, K.R.; Omens, J.H.; McCulloch, A.D. Anisotropic stretch-induced hypertrophy in neonatal ventricular myocytes micropatterned on deformable elastomers. *Biotechnol. Bioeng*. **2003**, *81*, 578-587.
14. Ahmed, W.W.; Wolfram, T.; Goldyn, A.M.; Bruellhoff, K.; Rioj, B.A.; Moller, M.; Spatz, J.P.; Saif, T.A.; Groll J.; Kemkemer, R. Myoblast morphology and organization on biochemically micro-patterned hydrogel coatings under cyclic mechanical strain. *Biomaterials* **2009**, *31*, 250-258.
15. Wang, N.; Ostuni, E.; Whitesides, G.M.; Ingber, D.E. Micropatterning tractional forces in living cells. *Cell Motil. Cytoskeleton* **2002**, *52*, 97-106.
16. Chen, C.S.; Jiang, X.; Whiteside, G.M. Microengineering the Environment of Mammalian Cells in Culture. *MRS Bull*. **2005**, *30*, 194-201.
17. Csucs, G.; Michel, R.; Lussi, J.W.; Textor, M.; Danuser, G. Microcontact printing of novel co-polymers in combination with proteins for cell-biological applications. *Biomaterials* **2003**, *24*, 1713-1720.
18. Park, H.S.; Lee, S.Y.; Yoon, H.; Noh, I. Biological evaluation of micro-patterned hyaluronic acid hydrogel for bone tissue engineering. *Pure Appl. Chem.* **2014**, *86*, 1911-1922.
19. Poellmann, M.J.; Harrell, P.A.; King, W.P.; Johnson, A.J.W. Geometric microenvironment directs cell morphology on topographically patterned hydrogel substrates. *Acta Biomater.* **2010**, *6*, 3514-3523.
20. Rape, A.D.; Guo, W.H.; Wang, Y.L. The regulation of traction force in relation to cell shape and focal adhesions. *Biomaterials* **2010**, *32*, 2043-2051.
21. Nelson, C.M.; Jean, R.P.; Tan, J.L.; Liu, W.F.; Sniadecki, N.J.; Spector, A.A; Chen, C.S. Emergent patterns of growth controlled by multicellular form and mechanics. *Proc. Natl. Acad. Sci. U. S. A*. **2005**, *102*, 11594-11599.
22. Ruiz, S.A.; Chen, C.S. Emergence of patterned stem cell differentiation within multicellular structures. *Stem Cells* **2008**, *26*, 2921-2927.
23. James, J.; Goluch, E.D.; Hu, H.; Liu, C.; Mrksich, M.; Subcellular curvature at the perimeter of micropatterned cells influences lamellipodial distribution and cell polarity. *Cell Motil. Cytoskeleton* **2008**, *65*, 841-852.

24. Théry, M.; Racine, V.; Piel, M.; Pépin, A.; Dimitrov, A.; Chen, Y.; Sibarita, J.B.; Bornens, M. Anisotropy of cell adhesive microenvironment governs cell internal organization and orientation of polarity. *Proc. Natl. Acad. Sci. U. S. A.* **2006**, *103*, 19771-19776.
25. Jiang, X.; Bruzewicz, D.A.; Wong, A.P.; Piel, M.; Whitesides, G.M. Directing cell migration with asymmetric micropatterns. *Proc. Natl. Acad. Sci. U. S. A*. **2005**, *102*, 975-978.
26. Mahmud, G.; Campbell, C.J.; Bishop, K.J.M.; Komarova, Y.A.; Chaga, O.; Soh, S.; Huda, S.; Kandere-Grzybowska, K.; Grzybowski, B.A. Directing cell motions on micropatterned ratchets. *Nat. Phys*. **2009**, *5*, 606-612.
27. Lee, K.Y.; Mooney, D.J. Hydrogels for Tissue Engineering. *Chem. Rev.* **2001**, *101*, 1869-1880.
28. Sidwell, R. U.; Dhillon, A. P.; Butler, P. E. M.; Rustin, M. H. A. Localized granulomatous reaction to a semi-permanent hyaluronic acid and acrylic hydrogel cosmetic filler. *Clin. Exp. Dermatol.* **2004**, 29, 630-632.
29. Lowe, N.J.; Maxwell, C.A.; Lowe, P.; Duickb, M.G.; Shah, K. Hyaluronic acid skin fillers: adverse reactions and skin testing. *J. Am. Acad. Dermatol.* **2011**, *45*, 930-933.
30. Mohabatpour, F.; Karkhaneh, A.; Sharifi, A.M. A hydrogel/fiber composite scaffold for chondrocyte encapsulation in cartilage tissue regeneration**.** *RSC Adv.* **2016**, *6*, 83135-83145.
31. Park, H.; Lee, H.J.; Ana, H.; Lee, K.Y. Alginate hydrogels modified with low molecular weight hyaluronate for cartilage regeneration. *Carbohydr. Polym.* **2017**, *162*, 100-107.
32. Sheikh, Z, Hamdan, N., Ikeda, Y, Grynpas, M, Ganss B. and Glogauer M. Natural graft tissues and synthetic biomaterials for periodontal and alveolar bone reconstructive applications: a review. *Biomater. Res.* **2017**, *21*:9.
33. Kim, M.H., Kim B.S., Lee, J., Cho, D., Kwon O. H. and Park W. H. Silk fibroin/hydroxyapatite composite hydrogel induced by gamma-ray irradiation for bone tissue engineering. *Biomater. Res.* **2017,** 21**:**12.
34. Ghosh, K.; Ren X.D.; Shu, X.Z.; Prestwich, G.D.; Clark, R.A. Fibronectin functional domains coupled to hyaluronan stimulate adult human dermal fibroblast responses critical for wound healing. *Tissue Eng.* **2006**, *12*, 601-613.
35. Gilli, R.; Kacurakova, M.; Mathlouthi, M.; Navarini, L.; Paoletti, S. FTIR studies of sodium hyaluronate and its oligomers in the amorphous solid phase and in aqueous solution. *Carbohydr. Res*. **1994**, *263*, 315-326.
36. Kim, D.; Park, H.J.; Lee, K.Y. Study on Curing Behaviors of Epoxy Acrylates by UV with and without Aromatic Component. *Macromol. Res*. **2015**, *23*, 944-951.
37. Cowman, M.K.; Hittner, D.M; Feder-Davis, J. $^{13}$C-NMR Studies of Hyaluronan: Conformational Sensitivity to Varied Environments. *Macromolecules* **1996**, *29*, 2894-2902.
38. Sheu, C.; Shalumon, K. T.; Chen, C.H.; Kuo, C.Y.; Fong, Y.T.; Chen, J.P. Dual cross-linked hyaluronic acid nanofibrous membranes for prolonged prevention of post-surgical peritoneal adhesion. *J. Mater. Chem. B* **2016**, *4*, 6680-6693.